

This work has been submitted to the IEEE for possible publication.
Copyright may be transferred without notice, after which this version may
no longer be accessible.

Robust Survivability-Oriented Scheduling of Separable Mobile Energy Storage and Demand Response for Isolated Distribution Systems

Wei Wang, *Student Member, IEEE*, Xiaofu Xiong, *Member, IEEE*, Yufei He, and Hongzhou Chen.

Abstract—Extreme circumstances in which a local distribution system is electrically isolated from the main power supply may not always be avoidable. Efforts must be made to keep the lights on for such an isolated distribution system (IDS) until reconnection to the main power source. In this paper, we propose a strategy to enhance IDS survivability utilizing the coordination of two flexible approaches, namely, separable energy storage systems (SMESs), which construct non-wires links for energy transmission between the IDS and the external live power sources, and demand response (DR), which adjusts the internal electrical demand of the IDS to provide effective operating stress alleviation. Considering the uncertainty of renewable energy generation and loads, a two-stage robust optimization (RO) model involving the joint scheduling of these two approaches is constructed. The objective is to minimize the fuel consumption rate and the decreased and nonserved demand under the worst-case scenario to endow the IDS with extended survivability. Finally, the test is conducted and the results demonstrate the effectiveness of the proposed method in enhancing the survivability of IDS.

Index Terms—Isolated distribution system, separable mobile energy storage systems, demand response, robust optimization.

NOMENCLATURE

Sets

T	Set of time spans of scheduling. $T = \{t 1 \leq t \leq D, t \in \mathcal{Z}\}$, where $D = T $ and \mathcal{Z} is set of integers.
$\mathcal{N}, \mathcal{N}_{\text{DR}}$	Set of nodes in the IDS and those participating in DR.
$\mathcal{S}, \mathcal{S}_s, \mathcal{S}_R$	Sets of external sources, such as a substation, and those as REG isolated from the IDS, respectively. $\mathcal{S} = \mathcal{S}_s \cup \mathcal{S}_R$.
\mathcal{N}_s	Set of nodes that support the access of SMESs, including those in the IDS and the external sources.
$\mathcal{F}(i)$	Set of FFGs located at node i in the IDS.
\mathcal{M}, \mathcal{K}	Sets of Carrs and Mods of SMESs.
\mathcal{L}	Set of branches in the IDS.

Variables

Ψ_{11}	Fuel consumption for SMESs' movement.
Ψ_{12}	Fuel consumption of FFGs.
Ψ_2	Total weighted energy demand reduced by DR during the scheduling.
Ψ_3	Total weighted nonpicked-up energy demand during the scheduling.
χ_i	Sum of the nonpicked-up power load at node i .
$x_{j,t}$	Binary variable, 1 if Carr j is parked at node i during time span t , 0 otherwise.
$v_{j,t}$	Binary variable, 1 if Carr j is traveling to node i during time span t , 0 otherwise.
$S_{j,t}$	Travel time to be consumed by Carr j during time span t .
$R_{j,t}$	Residual travel time of Carr j during time span t .
$\omega_{j,t}$	Binary variable, 1 if Carr j is traveling during time spans $t-1$ and t .
$\zeta_{k,i,t}$	Binary variable, 1 if Mod k belongs to node i during time span t , 0 otherwise.

$\gamma_{k,j,t}$	Binary variable, 1 if Mod k belongs to Carr j during time span t , 0 otherwise.
$\alpha_{j,i,k,t}$	Binary variable, 1 if Carr j carrying Mod k arrives at node i during time span t , 0 otherwise.
$c_{k,i,t}/d_{k,i,t}$	Binary variable, 1 if Mod k is charged/discharged at node i during time span t , 0 otherwise.
$P_{k,i,t}^S/P_{k,i,t}^{dS}$	Active power output of Mod k charged/discharged at node i during time span t .
$Q_{k,i,t}^S$	Reactive power output of Mod k charged/discharged at node i during time span t .
$SOC_{k,t}$	State of charge of Mod k at the end of time span t .
δ_i	Binary variable, 1 if the load at node i is picked up in the scheduling, 0 otherwise.
$\rho_{i,t}$	Binary variable, 1 if DR is executed at node i during time span t , 0 otherwise.
$P_{i,t}^{\text{DR}}$	Active load reduction due to DR execution at node i during time span t .
$C_{i,t}$	Accumulated energy (within a single DR execution) during time span t at node i .
$EP_{i,t}$	Energy about to rebound at node i after time span t .
$P_{i,t}^{\text{EP}}$	Net rebounded active load due to energy payback at node i during time span t .
$P_{i,t}^F/Q_{i,t}^F$	Active/reactive power output of FFG f during time span t .
$P_{i,t}^L/Q_{i,t}^L$	Active/reactive power load at node i due to scheduling during time span t .
$\tilde{P}_{i,t}^{\text{DL}}$	Original active power load at node i if it is picked up without DR during time span t .
$P_{i,t}^{\text{INS}}/Q_{i,t}^{\text{INS}}$	Active/reactive power input from SMESs at node i during time span t .
$\tilde{P}_{i,t}^{\text{REG}}$	Active power output at REG i out of the IDS during time span t .
$P_{i,t}^{\text{INF}}/Q_{i,t}^{\text{INF}}$	Active/reactive power input from FFGs at node i during time span t .
$P_{i',i}/Q_{i',i}$	Active/reactive power flow on branch (i', i) from node i' to node i during time span t .
$V_{i,t}^2$	Squared voltage magnitude at node i during time span t .
$\tilde{u}_{i,t}^+/\tilde{u}_{i,t}^-$	Upward/downward fluctuation of the original load at node i during time span t .
$\tilde{u}_{i,t}^{\text{REG}}/\tilde{u}_{i,t}^{\text{REG}}$	Upward/downward fluctuation of the power output of REG i during time span t .

Parameters

$\Psi_{1,\text{max}}$	Estimated possible upper bounds of total fuel consumption, energy demand reduced by DR and nonpicked-up energy demand, respectively.
$\Psi_{2,\text{max}}, \Psi_{3,\text{max}}$	Weight coefficients for Ψ_1, Ψ_2, Ψ_3 .
$\kappa_1, \kappa_2, \kappa_3$	Priority weight of the load at node i .
w_i	Unit fuel consumption for travel of Carr j and generation of FFG f .
μ_j, σ_j	Remaining fuel at the start of the scheduling.
$\hat{\psi}_1$	Length of a single time span.
Δt	A sufficiently large/small positive number.
M	Time spans spent traveling from node i to node i' for Carr j .
$T_{j,i,i'}$	Capacity consumed by Mod k .
W_k	Carrying capacity Carr j .
A_j	Maximum charging/discharging power and rated apparent power of Mod k .
$P_{k,\text{max}}^S/P_{k,\text{max}}^{dS}$	Energy capacity of Mod k .
$S_{k,\text{Mod}}$	Charging/discharging efficiency of Mod k .
E_k	
e_k^c/e_k^d	

$SOC_{k,min}/SOC_{k,max}$	Minimum/maximum allowable range of state of charge for Mod k .
$\tau_{i,min}^{DR}/\tau_{i,max}^{DR}$	Lower/upper bound of the ratio of load reduction due to DR execution at node i .
η_i	Ratio of the reactive load to the active load at node i .
$\rho'_{i,t}$	Record of whether DR was executed at node i or not during time span t in the previous scheduling.
$T_{i,DU,max}/T_{i,DU,min}$	Maximum/minimum allowable duration of a single DR execution at node i .
$T_{i,IN,min}$	Minimum allowable interval between two adjacent DR executions at node i .
$T_{i,DR,max}$	Maximum allowable total duration of DR executions at node i in the scheduling.
$C'_{i,t}, EP'_{i,t}$	Records of the accumulated energy and the energy about to rebound at node i during time span t in the previous scheduling.
$T_{i,pdu}$	Duration of an energy payback at node i .
$b_{i,h}$	Gain coefficient of energy payback on the active load during the h th time span in an energy payback.
$P_{f,max}^e/Q_{f,max}^e$	Maximum active/reactive power output and rated apparent power of FFG f .
$S_{f,FFG}^e$	Maximum charging power at substation i out of the IDS.
$P_{i,max}^{sub}$	Resistance/reactance of branch (i, i') .
$r_{ii'}/x_{ii'}$	Lower/upper bound of the voltage magnitude at node i .
$V_{i,min}/V_{i,max}$	Apparent power capacity of branch (i', i) .
$S_{i',max}$	Forecasted active power load and REG output at node i during time span t .
$\tilde{P}_{i,t}^{OL}, \tilde{P}_{i,t}^{REG}$	Maximum upward/downward fluctuation of the original load at node i .
$\Delta\tilde{P}_{i,t}^{OL}/\Delta\tilde{P}_{i,t}^{OL}$	Maximum upward/downward fluctuation of the power output of REG i .
$\Delta\tilde{P}_{i,t}^{REG}/\Delta\tilde{P}_{i,t}^{REG}$	

I. INTRODUCTION

CATASTROPHIC events over the past decades, *e.g.*, the 2008 Chinese winter storms, the 2012 Hurricane Sandy in the U.S., and the increasing reliance of society on electricity have raised awareness of the urgent demand and significance for enhancing power system resilience under high-impact, low-frequency (HILF) events [1]-[4]. A resilient power system, according to EPRI reports [1], [2], should 1) be hardened to limit damage, 2) quickly restore electric service, and 3) aid customers in continuing some level of service without access to normal power sources, referring to the three elements of resilience: *prevention*, *recovery*, and *survivability*, respectively.

In contrast to other parts of the power system, the distribution system (DS)'s greater exposure, complexity, and geographic reach result in greater vulnerability to most kinds of disruptions particularly HILF events that could cause widespread and long-term outages [1], [2]. To enhance DS resilience, extensive studies have been conducted on the first two elements. Regarding *prevention*, researchers have mainly focused on planning and reinforcement of facilities; and measures relating to line hardening [5], the allocation of energy resources such as energy storage and distributed generation [6], [7], automatic switch installation [8], and proactive islanding [9] have been studied. Among the research regarding *recovery*, which aims at restoring electric service of DS rapidly after the onset of HILF events, in addition to the well-allocated energy resources that can work soon to supply power to the de-energized targeted customers, measures involving the scheduling of mobile energy resources (*e.g.*, mobile energy storage systems (MESSs), mobile generators) [10], [11], repair crew [12], microgrids formation by DS reconfiguration [13], and demand response (DR) [14] have been shown to be effective. Enhanced situational awareness and precise damage assessment also make a large difference in DS recovery [15]. However, as we can see

from a review of the existing studies, while current research mainly focuses on addressing the demand for resilience enhancement from the aspects of *prevention* and *recovery*, little concern is given about the other aspect *survivability*, which focuses on the issue, according to EPRI [1], [2], about how the electric service to customers is sustained when the local DS is isolated from its normal sources, similar to the definition in [16]. Rather than aiming at restoring the lost loads rapidly as *recovery* does, in the authors' opinion, *survivability* emphasizes the performance of such an isolated DS (IDS) in sustaining the power supply to as many loads as possible until that isolation disappears, *i.e.*, until the IDS is reconnected to the grid.

In addition to the proactive islanding executed pre-emptively by the operator ahead of an HILF event [9], an IDS can be mainly formed by the forced outage of lines that link the DS and its normal source, *e.g.*, the substation, the renewable energy generation (REG) for geographically isolated areas such as remote islands [17]. Under this circumstance, the electricity fed by the external source to the IDS is blocked before the out-of-service lines that link them are repaired and resume running. That is, until the appearance of MESSs, which provides an alternative way to rebuild the lifeline by absorbing electricity from the external source and transporting and releasing it into the IDS. In our recent work [18], the idea of a separable MESS (SMESS) solution has been innovatively proposed, in which the energy storage modules (Mods) and the carriers (Carrs) of MESSs are scheduled as independent components to obtain extended flexibility. In this paper, the effectiveness of SMESSs in boosting the *survivability* of IDS is further studied. In addition, demand response (DR) is a flexible and useful tool to relieve the operating stress by adjusting the demand in the allowable range [14], [19], [20]. Typical applications are the "Emergency Demand Response Program (EDRP)" and the "Installed Capacity – Special Case Resources (ICAP/SCR) Program" administered by the New York Independent System Operator (NYISO) [21]. DR may work well to coordinate with the scheduling of SMESSs and operation of IDS and thus is also involved in our study herein. Based on the above description, a robust scheduling strategy is proposed to strengthen the IDS survivability. The main contributions are as follows:

1) A two-pronged strategy is developed to de-escalate the crises such as energy and power shortages suffered by the IDS. SMESSs successively transport energy from external sources to the IDS, and DR is executed inside to temporarily reduce the electricity demand to relieve the IDS' operating stress while taking into account the energy payback effect following DR.

2) Accordingly, a two-stage robust optimization (RO) model, involving the coordinated scheduling of SMESSs and DR and considering the uncertainty of renewable power generation (REG) output and loads, is formulated and solved by the column-and-constraint generation (C&CG) method.

The remainder of this paper is organized as follows. Section II provides a brief description of the survivability-oriented strategy; Section III proposes the two-stage RO model; Section IV describes the method to solve the model; Section V provides numerical studies; and finally, Section VI concludes this paper.

II. THE SURVIVABILITY-ORIENTED STRATEGY

A general scenario of IDS is shown in Fig. 1, where the local

area customers lose the continuous supply from the normal power sources (*i.e.*, the substation and the REG) but have back-up small-capacity fossil-fuel-based generation (FFG) within the IDS. In addition, we further assume such an extreme condition that limited fuel is stored in the IDS without any supplement from outside. This scenario can be simply revised to represent any other required scenarios, such as a case where an IDS, which is normally supplied only by the REG in a remote area, loses the supply from the REG by removing the substation node. The model in the following sections can also be simply revised accordingly. Then, a two-pronged strategy to enhance the survivability of the IDS is described as follows: 1) From the IDS's external point of view, SMESSs are scheduled to construct non-wires links for energy transmission from the outside "stranded" sources to the IDS. In addition, SMESSs can even realize a continuous power supply for the IDS, provided output of the Mods and traveling behavior of the CARRS are well scheduled. 2) From the IDS's internal point of view, DR is scheduled to relieve the energy and power shortages that may arise in the operation of IDS by reducing the demand in the allowable range. Considering that rapid response to the DR request from the IDS operator is beneficial and expected under such an emergency circumstance, in our strategy, the fully dispatchable DR is used, *e.g.*, direct load control (DLC), which can be executed directly by the operator, as in [14] and [19].

III. ROBUST SCHEDULING MODEL FORMULATION

A. Objective Function

The objective function in (1a) is to minimize the following three terms: 1) the total fuel consumed by CARRS for moving and FFGs for generation; 2) the customers' demand reduction due to DR; and 3) the demand not picked up, *i.e.*, the demand of the customers abandoned in the scheduling.

$$\min_{\mathbf{y}} \kappa_1 \frac{\Psi_{11}}{\Psi_{1,\max}} + \max_{\mathbf{u} \in \mathcal{U}} \min_x \kappa_1 \frac{\Psi_{12}}{\Psi_{1,\max}} + \kappa_2 \frac{\Psi_2}{\Psi_{2,\max}} + \kappa_3 \frac{\Psi_3}{\Psi_{3,\max}} \quad (1a)$$

where \mathbf{y} represents the first-stage decision variables regarding the traveling behaviors of SMESSs and the states of picking up nodes and executing DR and expressed as $\mathbf{y} = \{x_{j,i,t}, v_{j,i,t}, S_{j,t}, R_{j,t}, \omega_{j,t}, \zeta_{k,i,t}, \gamma_{k,j,t}, \alpha_{j,i,k,t}, c_{k,i,t}, d_{k,i,t}, \delta_i, \rho_{i,t}, \Psi_{11}\}$; $\mathbf{u} = \{\tilde{P}_{i,t}^{\text{OL}}, \tilde{P}_{i,t}^{\text{REG}}\}$ represents the uncertain loads and REG outputs; $\mathcal{U} = \{\mathcal{U}_L, \mathcal{U}_{\text{REG}}\}$; and the second-stage variable \mathbf{x} contains the rest of the variables except those in the uncertainty sets. κ_1 , κ_2 and κ_3 can be determined by decision-makers' preference or the analytic hierarchic process (AHP) [12]. $\Psi_{1,\max}$, $\Psi_{2,\max}$, and $\Psi_{3,\max}$ are introduced for normalization and can be estimated as: $\Psi_{1,\max} = \sum_{i \in \mathcal{T}} (\sum_{j \in \mathcal{M}} \mu_j \Delta t + \sum_{i \in \{i | \mathcal{F}(i) \neq \emptyset\}} \sum_{f \in \mathcal{F}(i)} \sigma_f P_{f,\max}^F \Delta t)$, $\Psi_{2,\max} = \sum_{i \in \mathcal{N}_{\text{DR}}} w_i \tau_{i,\max}^{\text{DR}} (\max_{i \in \mathcal{T}} \tilde{P}_{i,t}^{\text{OL}}) T_{i,\text{DR},\max} \Delta t$, and $\Psi_{3,\max} = \sum_{i \in \mathcal{N}} w_i \sum_{i \in \mathcal{T}} \tilde{P}_{i,t}^{\text{OL}} \Delta t$.

The following constraints express the terms in (1):

$$\Psi_{11} = \sum_{i \in \mathcal{T}} \sum_{j \in \mathcal{M}} \mu_j \sum_{i \in \mathcal{N}} v_{j,i,t} \Delta t \quad (2a)$$

$$\Psi_{12} = \sum_{i \in \mathcal{T}} \sum_{i \in \{i | \mathcal{F}(i) \neq \emptyset\}} \sum_{f \in \mathcal{F}(i)} \sigma_f P_{f,t}^F \Delta t \quad (2b)$$

$$\Psi_{11} + \Psi_{12} \leq \tilde{\Psi}_1 \quad (2c)$$

$$\Psi_2 = \sum_{i \in \mathcal{T}} \sum_{i \in \mathcal{N}_{\text{DR}}} w_i P_{i,t}^{\text{DR}} \Delta t \quad (2d)$$

$$-M \delta_i \leq \chi_i - \sum_{i \in \mathcal{T}} \tilde{P}_{i,t}^{\text{OL}} \leq 0, \quad 0 \leq \chi_i \leq M(1 - \delta_i), \quad \forall i \in \mathcal{N} \quad (2e)$$

$$\Psi_3 = \sum_{i \in \mathcal{N}} w_i \chi_i \Delta t \quad (2f)$$

We assume for simplicity that the same type of fuel (*e.g.*,

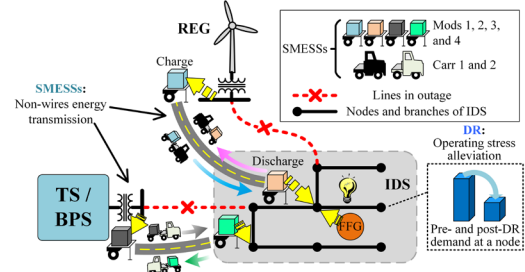


Fig. 1. Illustration of "Keeping the lights on" for an IDS via SMESSs and DR. diesel) is consumed by transportation of CARRS and operation of FFGs, as expressed by (2c). Thus, the same weight is adopted for Ψ_{11} and Ψ_{12} , both of which means the fuel consumption.

B. Constraints for SMESSs

The constraints for the scheduling of SMESSs, first proposed in our recent work [18], are used herein, formulated as follows.

$$\sum_{i \in \mathcal{N}_S} x_{j,i,t} + \sum_{i \in \mathcal{N}_S} v_{j,i,t} = 1, \quad \forall t \in \mathcal{T} \cup \{0\}, j \in \mathcal{M} \quad (3a)$$

$$\begin{cases} x_{j,i,t} \geq x_{j,i,t-1} + 1.2(v_{j,i,t-1} - v_{j,i,t}) + 0.4(\sum_{i \in \mathcal{N}_S} v_{j,i,t-1} - \sum_{i \in \mathcal{N}_S} v_{j,i,t}) - 0.8 \\ x_{j,i,t} \leq x_{j,i,t-1} + (v_{j,i,t-1} - v_{j,i,t}) - 0.5(\sum_{i \in \mathcal{N}_S} v_{j,i,t-1} - \sum_{i \in \mathcal{N}_S} v_{j,i,t}) + 0.7 \end{cases} \quad (3b)$$

, $\forall t \in \mathcal{T}, j \in \mathcal{M}, i \in \mathcal{N}_S$

$$\begin{cases} S_{j,t} \geq x_{j,i,t-1} \sum_{i \in \mathcal{N}_S} T_{j,i,t} + \sum_{i \in \mathcal{N}_S} (v_{j,i,t} T_{j,i,t}) - \sum_{i \in \mathcal{N}_S} T_{j,i,t}, \quad \forall i \in \mathcal{N}_S \\ S_{j,t} \geq 0 \end{cases} \quad (3c)$$

, $\forall t \in \mathcal{T}, j \in \mathcal{M}$

$$R_{j,t} = R_{j,t-1} + S_{j,t} - \sum_{i \in \mathcal{N}_S} v_{j,i,t-1}, \quad \forall t \in \mathcal{T}, j \in \mathcal{M} \quad (3d)$$

$$R_{j,t} / M \leq \sum_{i \in \mathcal{N}_S} v_{j,i,t} \leq R_{j,t}, \quad \forall t \in \mathcal{T}, j \in \mathcal{M} \quad (3e)$$

$$\begin{cases} \omega_{j,t} \geq \sum_{i \in \mathcal{N}_S} v_{j,i,t-1} + \sum_{i \in \mathcal{N}_S} v_{j,i,t} - 2 + \varepsilon \\ -(1 - \omega_{j,t}) \leq v_{j,i,t} - v_{j,i,t-1} \leq (1 - \omega_{j,t}), \quad \forall i \in \mathcal{N}_S \end{cases} \quad (3f)$$

, $\forall t \in \mathcal{T}, j \in \mathcal{M}$

$$x_{j,i,0} = 1, S_{j,0} = 0, R_{j,0} = 0, \omega_{j,0} = 0, \quad \forall j \in \mathcal{M} \quad (3g)$$

$$\sum_{i \in \mathcal{N}_S} \zeta_{k,i,t} + \sum_{j \in \mathcal{M}} \gamma_{k,j,t} = 1, \quad \forall t \in \mathcal{T} \cup \{0\}, k \in \mathcal{K} \quad (4a)$$

$$\sum_{k \in \mathcal{K}} W_k \gamma_{k,j,t} \leq A_j, \quad \forall t \in \mathcal{T} \cup \{0\}, j \in \mathcal{M} \quad (4b)$$

$$\zeta_{k,i,0} = 1, \quad \forall k \in \mathcal{K} \quad (4c)$$

$$\gamma_{k,j,t} \leq 1 - \sum_{i \in \mathcal{N}_S} x_{j,i,t}, \quad \forall t \in \mathcal{T} \cup \{0\}, j \in \mathcal{M}, k \in \mathcal{K} \quad (4d)$$

$$\gamma_{k,j,t} - \zeta_{k,i,t-1} \leq x_{j,i,t} + 1 - x_{j,i,t-1}, \quad \forall t \in \mathcal{T}, j \in \mathcal{M}, i \in \mathcal{N}_S, k \in \mathcal{K} \quad (4e)$$

$$-\left(\sum_{i \in \mathcal{N}_S} x_{j,i,t-1} + \sum_{i \in \mathcal{N}_S} x_{j,i,t}\right) \leq \gamma_{k,j,t} - \gamma_{k,j,t-1} \leq \sum_{i \in \mathcal{N}_S} x_{j,i,t-1} + \sum_{i \in \mathcal{N}_S} x_{j,i,t}, \quad \forall t \in \mathcal{T}, j \in \mathcal{M}, k \in \mathcal{K} \quad (4f)$$

$$\begin{cases} \alpha_{j,i,k,t} \leq 1 - x_{j,i,t-1}; \alpha_{j,i,k,t} \leq x_{j,i,t}; \\ \alpha_{j,i,k,t} \leq \gamma_{k,j,t-1}; \alpha_{j,i,k,t} \geq -x_{j,i,t-1} + x_{j,i,t} + \gamma_{k,j,t-1} - 1 \end{cases} \quad (4g)$$

, $\forall t \in \mathcal{T}, i \in \mathcal{N}_S, j \in \mathcal{M}, k \in \mathcal{K}$

$$\zeta_{k,i,t} \geq \sum_{j \in \mathcal{M}} \alpha_{j,i,k,t}, \quad \forall t \in \mathcal{T}, i \in \mathcal{N}_S, k \in \mathcal{K} \quad (4h)$$

$$\zeta_{k,i,t} - \zeta_{k,i,t-1} \leq \sum_{j \in \mathcal{M}} \alpha_{j,i,k,t}, \quad \forall t \in \mathcal{T}, i \in \mathcal{N}_S, k \in \mathcal{K} \quad (4i)$$

$$c_{k,i,t} + d_{k,i,t} \leq \zeta_{k,i,t}, \quad \forall t \in \mathcal{T}, k \in \mathcal{K}, i \in \mathcal{N}_S \quad (5)$$

$$0 \leq P_{k,i,t}^{e,S} \leq c_{k,i,t} P_{k,\max}^{e,S}, \quad 0 \leq P_{k,i,t}^{d,S} \leq d_{k,i,t} P_{k,\max}^{d,S}, \quad (6a)$$

$$-S_{k,\text{Mod}} \zeta_{k,i,t} \leq Q_{k,i,t}^S \leq S_{k,\text{Mod}} \zeta_{k,i,t}, \quad \forall t \in \mathcal{T}, k \in \mathcal{K}, i \in \mathcal{N}_S$$

$$\left[\sum_{i \in \mathcal{N}_S} (P_{k,i,t}^{d,S} - P_{k,i,t}^{e,S})\right]^2 + \left(\sum_{i \in \mathcal{N}_S} Q_{k,i,t}^S\right)^2 \leq S_{k,\text{Mod}}^2, \quad \forall t \in \mathcal{T}, k \in \mathcal{K} \quad (6b)$$

$$SOC_{k,t} = SOC_{k,t-1} + \left(e_k^c \sum_{i \in \mathcal{N}_S} P_{k,i,t}^{c,S} - \sum_{i \in \mathcal{N}_S} P_{k,i,t}^{d,S} / e_k^d \right) \Delta t / E_k, \quad (6c)$$

$$SOC_{k,\min} \leq SOC_{k,t} \leq SOC_{k,\max}, \quad \forall t \in \mathcal{T}, k \in \mathcal{K}$$

Specific descriptions of most of the constraints are listed in Table I. The detailed derivations of (3) and (4) can be found in our prior works [22] and [18].

C. Constraints for DR

The constraints for DR are formulated as follows. In addition, a DR event is commonly followed by a temporary rebound of the load, referred to as the energy payback effect, which can result from that, *e.g.*, the heating or air conditioning equipment tending to use extra energy to remove the heat gained during the reduced service levels [19], [23]. The energy payback effect following the end of each DR event is considered in this paper.

$$\rho_{i,t} \leq \delta_i, \quad \forall i \in \mathcal{N}_{DR}, t \in \mathcal{T} \quad (7a)$$

$$\begin{cases} 0 \leq P_{i,t}^{DR} \leq M \rho_{i,t} \\ P_{i,t}^{DR} \leq \tau_{i,\max}^{DR} \tilde{P}_{i,t}^{OL} \\ \tau_{i,\min}^{DR} \tilde{P}_{i,t}^{OL} - P_{i,t}^{DR} \leq M(1 - \rho_{i,t}) \end{cases}, \quad \forall i \in \mathcal{N}_{DR}, t \in \mathcal{T} \quad (7b)$$

$$\rho_{i,t} = \rho'_{i,D+t}, \quad \forall i \in \mathcal{N}_{DR}, t \in \{t \mid h \leq t \leq 0, t \in \mathcal{Z}\},$$

$$\text{where } h = \min\{-T_{i,DU,\max} + 1, -T_{i,IN,\min} + 1\} \quad (7c)$$

$$\sum_{h=0}^{T_{i,DU,\max}} \rho_{i,t+h} \leq T_{i,DU,\max}, \quad \forall i \in \mathcal{N}_{DR},$$

$$t \in \{t \mid -T_{i,DU,\max} + 1 \leq t \leq D - T_{i,DU,\max}, t \in \mathcal{Z}\} \quad (7d)$$

$$\sum_{h=0}^{T_{i,DU,\min}-1} \rho_{i,t+h} \geq (\rho_{i,t} - \rho_{i,t-1}) T_{i,DU,\min}, \quad \forall i \in \mathcal{N}_{DR},$$

$$t \in \{t \mid -T_{i,DU,\min} + 2 \leq t \leq D - T_{i,DU,\min} + 1, t \in \mathcal{Z}\} \quad (7e)$$

$$\sum_{h=0}^{T_{i,IN,\min}-1} (1 - \rho_{i,t+h}) \geq (\rho_{i,t-1} - \rho_{i,t}) T_{i,IN,\min}, \quad \forall i \in \mathcal{N}_{DR},$$

$$t \in \{t \mid -T_{i,IN,\min} + 2 \leq t \leq D - T_{i,IN,\min} + 1, t \in \mathcal{Z}\} \quad (7f)$$

$$\sum_{t \in \mathcal{T}} \rho_{i,t} \leq T_{i,DR,\max}, \quad \forall i \in \mathcal{N}_{DR} \quad (7g)$$

$$\begin{cases} 0 \leq C_{i,t} \leq M \rho_{i,t} \\ -M(1 - \rho_{i,t}) \leq C_{i,t} - (C_{i,t-1} + P_{i,t}^{DR}) \leq 0, \quad \forall i \in \mathcal{N}_{DR}, t \in \mathcal{T} \\ C_{i,0} = C'_{i,D} \end{cases} \quad (8a)$$

$$\begin{cases} -M \rho_{i,t+1} \leq EP_{i,t} - C_{i,t} \leq 0 \\ 0 \leq EP_{i,t} \leq M(1 - \rho_{i,t+1}) \end{cases}, \quad \forall i \in \mathcal{N}_{DR}, t \in \{\mathcal{T} \setminus \{D\}\} \cup \{0\} \quad (8b)$$

$$EP_{i,t} = EP'_{i,D+t}, \quad \forall i \in \mathcal{N}_{DR}, t \in \{t \mid -T_{i,pdu} + 1 \leq t \leq -1, t \in \mathcal{Z}\} \quad (8c)$$

$$P_{i,t}^{EP} = \sum_{h=1}^{T_{i,pdu}} b_h EP_{i,t-h}, \quad \forall i \in \mathcal{N}_{DR}, t \in \mathcal{T} \quad (8d)$$

As indicated by δ_i , we assume that in each scheduling, rather than all the loads that must be supplied, the IDS operator can determine which load is picked up or abandoned. In addition, the link between the current and the previous schedulings is considered, as expressed by (7c) and (8c). This is necessary because, for example, if a DR was still being executed at the end of the previous scheduling, then it must be considered in the current scheduling to ensure that the total duration of this DR, which may cross the two adjacent scheduling horizons, is within its allowable range. Constraints (8) express the energy payback effect. As shown in Fig. 2, “ $C_{i,t}$ ” accumulates the reduced energy consumption during a single DR execution, and “ $EP_{i,t}$ ” identifies the total accumulated one at the end of the DR, part or all of which is about to rebound back into the customer’s post-DR demand in the subsequent period of $T_{i,pdu}$. Typically, a

TABLE I
MEANINGS OF CONSTRAINTS (3) TO (16)

Constraint/c onstraints	Meaning/purpose
(3a)	A Carr has the only state during each time span in the scheduling.
(3b)	Restrict the state transitions of the CARRs.
(3c), (3d)	Derive the required travel time from the current states of the CARRs.
(3e)	A Carr must be traveling if the required travel time is not yet spent up.
(3f)	Maintain the direction during each travel.
(3g)	Set the initial state, <i>i.e.</i> , Carr j is initially located at node i_j .
(4a)	A Mod has the only location during each time span in the scheduling
(4b)	Restrict the carrying capacity of the CARRs.
(4c)	Set the initial state, <i>i.e.</i> , Mod k is initially located at node i_k .
(4d)	A Carr does not own any Mod when it is parked at a node, based on the assumption that a node always dominate all the Mods located at it.
(4e)	A Carr can carry away some of the Mods when it departs from there.
(4f)	The state of any Mod regarding a Carr cannot be changed when the Carr is traveling.
(4g)	Introduce and define binary variables $o_{j,i,k,t}$.
(4h), (4i)	If there is a Carr carrying a Mod to one node, then this node obtains this Mod; otherwise, this node cannot obtain it, or may lose it if this Mod has been already located there.
(5)	A Mod can be charged or discharged only while it is located at a node.
(6a), (6b)	Restrict the active/reactive power output of the Mods.
(6c)	Restrict the SOC of the Mods.
(7a)	DR can be executed at a node only if this node is picked up.
(7b)	Restrict the amount of load reduction due to DR.
(7c), (8c)	Build the link between the previous scheduling and the current one.
(7d), (7e)	Bound the allowable duration of single DR execution.
(7f)	Bound the allowable interval between two adjacent DR executions.
(7g)	Bound the total allowable duration of DR executions in scheduling.
(8a)	Accumulate the reduced energy consumption during a single DR.
(8b)	Identify the total reduced energy consumption due to a DR execution.
(8d)	Express the effect of energy payback on the actual load.
(9a), (9b)	Restrict the active/reactive power output of the FFGs.
(10a), (10b)	Express the power load in the IDS due to scheduling.
(11a), (11b)	Express the power input from SMESSES.
(11c), (11d)	Bound the power absorbed from external sources by SMESSES.
(12a), (12b)	Express the power input from FFGs.
(13)	Ensure power balance at nodes of the IDS.
(14)	Express the voltage relationship between two adjacent nodes.
(15)	Bound the voltage magnitude at nodes of the IDS.
(16)	Constrain the power flow on branches of the IDS.

100% payback can be applied to residential customers and 50% to commercial and industrial customers [19], which implies that $\sum_{h=1}^{\lceil T_{pdu}/\Delta t \rceil} b_h$ is equal to 1 and 0.5, respectively.

D. Constraints for FFGs

$$\begin{cases} 0 \leq P_{f,t}^F \leq P_{f,\max}^F \\ 0 \leq Q_{f,t}^F \leq Q_{f,\max}^F \end{cases}, \quad \forall f \in \bigcup_{i \in \mathcal{N}} \mathcal{F}(i), t \in \mathcal{T} \quad (9a)$$

$$(P_{f,t}^F)^2 + (Q_{f,t}^F)^2 \leq S_{f,FFG}^2, \quad \forall f \in \bigcup_{i \in \mathcal{N}} \mathcal{F}(i), t \in \mathcal{T} \quad (9b)$$

E. Constraints for IDS

The constraints for IDS operation are formulated as follows based on the linearized DistFlow model [10], [12], [24].

$$\begin{cases} -M(1 - \delta_i) \leq P_{i,t}^L - (\tilde{P}_{i,t}^{OL} - P_{i,t}^{DR} + P_{i,t}^{EP}) \leq 0, \\ \forall i \in \mathcal{N}_{DR}, \\ -M(1 - \delta_i) \leq P_{i,t}^L - \tilde{P}_{i,t}^{OL} \leq 0, \quad \forall i \in \mathcal{N} \setminus \mathcal{N}_{DR}, \\ 0 \leq P_{i,t}^L \leq M \delta_i, \quad \forall i \in \mathcal{N} \end{cases}, \quad \forall t \in \mathcal{T} \quad (10a)$$

$$Q_{i,t}^L = \eta_{i,t} P_{i,t}^L, \quad \forall i \in \mathcal{N}, t \in \mathcal{T} \quad (10b)$$

$$P_{i,t}^{IN,S} = \sum_{k \in \mathcal{K}} (P_{k,i,t}^{d,S} - P_{k,i,t}^{c,S}), \quad Q_{i,t}^{IN,S} = \sum_{k \in \mathcal{K}} Q_{k,i,t}^S,$$

$$\forall i \in \mathcal{N}_S, t \in \mathcal{T} \quad (11a)$$

$$P_{i,t}^{IN,S} = 0, \quad Q_{i,t}^{IN,S} = 0, \quad \forall i \in \{\mathcal{N} \cup \mathcal{S}\} \setminus \mathcal{N}_S, t \in \mathcal{T} \quad (11b)$$

$$-P_{i,t}^{IN,S} \leq P_{i,\max}^{sub}, \quad \forall i \in \mathcal{S}_S, t \in \mathcal{T} \quad (11c)$$

$$-P_{i,t}^{IN,S} \leq \tilde{P}_{i,t}^{REG}, \quad \forall i \in \mathcal{S}_R, t \in \mathcal{T} \quad (11d)$$

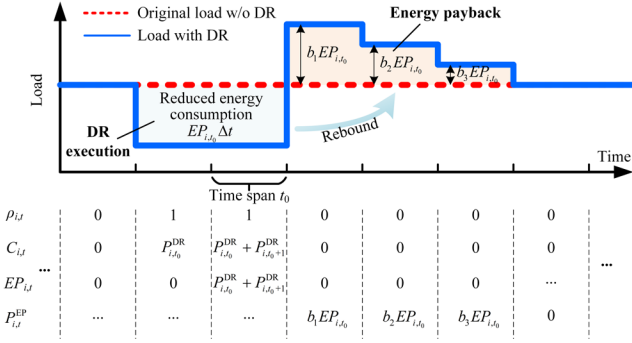


Fig. 2. Illustration about the effect of energy payback and how constraints (8) work. $T_{i,pdu}=3\Delta t$ is assumed.

$$P_{i,t}^{IN,F} = \sum_{f \in \mathcal{F}(i)} P_{f,t}^F, \quad Q_{i,t}^{IN,F} = \sum_{f \in \mathcal{F}(i)} Q_{f,t}^F$$

$$\forall i \in \{i | \mathcal{F}(i) \neq \Phi\}, t \in \mathcal{T} \quad (12a)$$

$$P_{i,t}^{IN,F} = 0, \quad Q_{i,t}^{IN,F} = 0, \quad \forall i \in \{i | \mathcal{F}(i) = \Phi\}, t \in \mathcal{T} \quad (12b)$$

$$\sum_{(i',i) \in \mathcal{L}} P_{i',t} + P_{i,t}^{INS} + P_{i,t}^{IN,F} - P_{i,t}^L = \sum_{(i',i) \in \mathcal{L}} P_{i',t}^F, \quad (13)$$

$$\sum_{(i',i) \in \mathcal{L}} Q_{i',t} + Q_{i,t}^{INS} + Q_{i,t}^{IN,F} - Q_{i,t}^L = \sum_{(i',i) \in \mathcal{L}} Q_{i',t}^F, \quad \forall i \in \mathcal{N}, t \in \mathcal{T} \quad (14)$$

$$V_{i,t}^2 = V_{i,t}^2 - 2(P_{i',t} r_{i',t} + Q_{i',t} x_{i',t}), \quad \forall (i, i') \in \mathcal{L}, t \in \mathcal{T} \quad (14)$$

$$V_{i,\min}^2 \leq V_{i,t}^2 \leq V_{i,\max}^2, \quad \forall i \in \mathcal{N}, t \in \mathcal{T} \quad (15)$$

$$P_{i',t}^2 + Q_{i',t}^2 \leq S_{i',\max}^2, \quad \forall (i, i') \in \mathcal{L}, t \in \mathcal{T} \quad (16)$$

F. Uncertainty Sets

The uncertainty sets of the REGs' power outputs and the IDSs' loads are given as (17), where the budgets of uncertainty, Γ_i^L and Γ_i^{REG} , provide a trade-off between the robustness and the conservatism of the solution [25]. When all the budgets are equal to 0, a deterministic model without considering any uncertainty is obtained; as the budgets increase, the uncertainty set is enlarged, and the resultant solution is thus increasingly conservative. We follow [26] and assume the budgets as integer.

$$\mathcal{U}_L = \left\{ \begin{array}{l} \tilde{P}_{i,t}^{\text{OL}} = \bar{P}_{i,t}^{\text{OL}} + \tilde{u}_{i,t}^{\text{OL}} \Delta \tilde{P}_{i,t}^{\text{OL}} - \tilde{u}_{i,t}^{\text{OL}} \Delta \tilde{P}_{i,t}^{\text{OL}}, \\ 0 \leq \tilde{u}_{i,t}^{\text{OL}} \leq 1, 0 \leq \tilde{u}_{i,t}^{\text{OL}} \leq 1, \forall i \in \mathcal{N}, t \in \mathcal{T} \\ \sum_{t \in \mathcal{T}} (\tilde{u}_{i,t}^{\text{OL}} + \tilde{u}_{i,t}^{\text{OL}}) \leq \Gamma_i^L, \forall i \in \mathcal{N} \end{array} \right\} \quad (17a)$$

$$\mathcal{U}_{\text{REG}} = \left\{ \begin{array}{l} \tilde{P}_{i,t}^{\text{REG}} = \bar{P}_{i,t}^{\text{REG}} + \tilde{u}_{i,t}^{\text{REG}} \Delta \tilde{P}_{i,t}^{\text{REG}} - \tilde{u}_{i,t}^{\text{REG}} \Delta \tilde{P}_{i,t}^{\text{REG}}, \\ 0 \leq \tilde{u}_{i,t}^{\text{REG}} \leq 1, 0 \leq \tilde{u}_{i,t}^{\text{REG}} \leq 1, \forall i \in \mathcal{S}_R, t \in \mathcal{T} \\ \sum_{t \in \mathcal{T}} (\tilde{u}_{i,t}^{\text{REG}} + \tilde{u}_{i,t}^{\text{REG}}) \leq \Gamma_i^{\text{REG}}, \forall i \in \mathcal{S}_R \end{array} \right\} \quad (17b)$$

The quadratic terms in (6b), (9b) and (16) can be converted into linear forms (see [26]). Thus, all the constraints are linear.

IV. SOLUTION METHODOLOGY

The two-stage RO model (1)-(17) can be expressed as the following compact form and solved by the C&CG method [27].

$$\min_y \mathbf{c}_{\text{out}}^T \mathbf{y} + \max_{\mathbf{u} \in \mathcal{U}} \min_x \mathbf{c}_{\text{in}}^T \mathbf{x} \quad (17)$$

$$\text{s.t.} \quad \mathbf{A} \mathbf{y} \leq \mathbf{B} \quad (18)$$

$$\mathbf{A}_{\text{eq}} \mathbf{y} = \mathbf{B}_{\text{eq}} \quad (19)$$

$$\mathbf{D} \mathbf{y} + \mathbf{E} \mathbf{x} + \mathbf{F} \mathbf{u} \leq \mathbf{G} \quad (20)$$

$$\mathbf{D}_{\text{eq}} \mathbf{y} + \mathbf{E}_{\text{eq}} \mathbf{x} = \mathbf{G}_{\text{eq}} \quad (21)$$

Based on the C&CG method, the model can be solved by iteratively solving the updated master problem and subproblem.

Algorithm 1 C&CG method to solve (17)-(21).

Step 1: At first, set $lb(0)=-\infty$ and $ub(0)=+\infty$. Set ε small enough.

Step 2: Solve **MP** and obtain the optimal solution $\{\mathbf{y}_k^*, \boldsymbol{\eta}_k^*\}$. Set the lower bound $lb(k)=\mathbf{c}_{\text{out}}^T \mathbf{y}_k^* + \boldsymbol{\eta}_k^*$. Specially for $k=1$, we can solve **MP** without considering $\boldsymbol{\eta}$ and (22)-(24).

Step 3: Substitute \mathbf{y}_k^* into **SP2** and solve it after handling with the bilinear terms as described above. Obtain the optimal solution $\{\mathbf{x}_k^*, \mathbf{u}_k^*\}$. Set the upper bound $ub(k)=\min\{ub(k-1), \mathbf{c}_{\text{out}}^T \mathbf{y}_k^* + \mathbf{c}_{\text{in}}^T \mathbf{x}_k^*\}$.

Step 4: If $ub(k)-lb(k)<\varepsilon$, then the solving process is completed and return the results. If not, go to **Step 5**.

Step 5: Create variable \mathbf{x}^k and add the constraints $\boldsymbol{\eta} \geq \mathbf{c}_{\text{in}}^T \mathbf{x}^k, \mathbf{D} \mathbf{y} + \mathbf{E} \mathbf{x}^k + \mathbf{F} \mathbf{u}_k^* \leq \mathbf{G}$, and $\mathbf{D}_{\text{eq}} \mathbf{y} + \mathbf{E}_{\text{eq}} \mathbf{x}^k = \mathbf{G}_{\text{eq}}$ to **MP**. Then, $k=k+1$ and go to **Step 2**.

Specifically, the master problem in the k th iteration is

$$\text{MP:} \quad \min_y \mathbf{c}_{\text{out}}^T \mathbf{y} + \boldsymbol{\eta} \quad (18), (19)$$

$$\text{s.t.} \quad \boldsymbol{\eta} \geq \mathbf{c}_{\text{in}}^T \mathbf{x}^l, \quad l=1, 2, \dots, k-1 \quad (22)$$

$$\mathbf{D} \mathbf{y} + \mathbf{E} \mathbf{x}^l + \mathbf{F} \mathbf{u}_l^* \leq \mathbf{G}, \quad l=1, 2, \dots, k-1 \quad (23)$$

$$\mathbf{D}_{\text{eq}} \mathbf{y} + \mathbf{E}_{\text{eq}} \mathbf{x}^l = \mathbf{G}_{\text{eq}}, \quad l=1, 2, \dots, k-1 \quad (24)$$

where \mathbf{u}_l^* is the optimal scenario (i.e., \mathbf{u}_l^* represents the worst case) obtained by solving the subproblem in the l th iteration.

After obtaining the optimal \mathbf{y}_k^* by solving the above **MP**, the subproblem can be written as:

$$\text{SP1:} \quad \max_{\mathbf{u} \in \mathcal{U}} \min_x \mathbf{c}_{\text{in}}^T \mathbf{x} \quad (25)$$

$$\text{s.t.} \quad \mathbf{D} \mathbf{y}_k^* + \mathbf{E} \mathbf{x} + \mathbf{F} \mathbf{u} \leq \mathbf{G} \quad (26)$$

$$\mathbf{D}_{\text{eq}} \mathbf{y}_k^* + \mathbf{E}_{\text{eq}} \mathbf{x} = \mathbf{G}_{\text{eq}} \quad (27)$$

To solve **SP1**, we can equivalently convert the inner linear minimization problem to its dual form based on the strong duality theorem, and then we rewrite **SP1** as

$$\text{SP2:} \quad \max_{\boldsymbol{\lambda}_1, \boldsymbol{\lambda}_2, \mathbf{u}} \boldsymbol{\lambda}_1^T (\mathbf{G} - \mathbf{D} \mathbf{y}_k^* - \mathbf{F} \mathbf{u}) + \boldsymbol{\lambda}_2^T (\mathbf{G}_{\text{eq}} - \mathbf{D}_{\text{eq}} \mathbf{y}_k^*) \quad (28)$$

$$\text{s.t.} \quad \boldsymbol{\lambda}_1^T \mathbf{E} + \boldsymbol{\lambda}_2^T \mathbf{E}_{\text{eq}} = \mathbf{c}_{\text{in}}^T \quad (29)$$

$$\boldsymbol{\lambda}_1 \leq 0 \quad (30)$$

$$\mathbf{u} \in \mathcal{U} \quad (31)$$

where $\boldsymbol{\lambda}_1$ and $\boldsymbol{\lambda}_2$ are dual variables of the inner problem of **SP1**.

Note that the bilinear term $\boldsymbol{\lambda}_1 \cdot \mathbf{u}$, more specifically, the terms $\lambda_1(n) \cdot \tilde{u}_{i,t}^L, \lambda_1(n) \cdot \tilde{u}_{i,t}^{\text{REG}}, \dots$ where $\lambda_1(n)$ is the n th element of $\boldsymbol{\lambda}_1$ if we substitute (17) into (28), makes **SP2** still hard to solve. However, for bilinear programming **SP2**, there exists an optimal solution lying at a vertex of its feasible region [28]. Thus, we can set the budgets Γ_i^L and Γ_i^{REG} in (17) as integers and then the optimal $\tilde{u}_{i,t}^L, \tilde{u}_{i,t}^{\text{REG}},$ and $\tilde{u}_{i,t}^{\text{REG}}$ belong to $\{0, 1\}$, as proved in [29]. From this, we define $\hat{u}_{i,t}^L, \hat{u}_{i,t}^L, \hat{u}_{i,t}^{\text{REG}},$ and $\hat{u}_{i,t}^{\text{REG}}$ as binary variables and the bilinear terms in (28) can be converted to linear forms by introducing new variables and adding new constraints to **SP2**, as in [26]. For example, for $\lambda_1(n) \cdot \hat{u}_{i,t}^L$, we can introduce a new variable $\hat{z}_{n,i,t}^L$ to replace $\lambda_1(n) \cdot \hat{u}_{i,t}^L$ in (28) and add the following constraints to **SP2**:

$$-M(1 - \hat{u}_{i,t}^L) \leq \hat{z}_{n,i,t}^L - \lambda_1(n) \leq M(1 - \hat{u}_{i,t}^L),$$

$$-M \hat{u}_{i,t}^L \leq \hat{z}_{n,i,t}^L \leq -M \hat{u}_{i,t}^L \quad (32)$$

Finally, both **MP** and **SP2** are mixed-integer linear programmings (MILPs) and can be solved by off-the-shelf solvers. The specific C&CG method is given as Algorithm 1.

V. NUMERICAL RESULTS

In this section, we conduct case studies to verify the effectiveness of the proposed model. The modified IEEE 33-

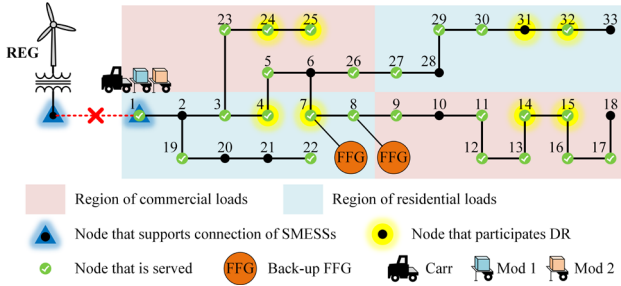


Fig. 3. The test system.

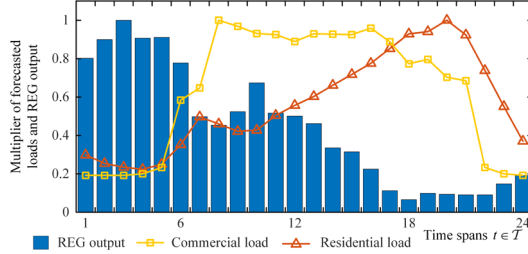


Fig. 4. The test system.

TABLE II

SPECIFIC PARAMETERS ADOPTED IN THE TEST

SPECIFIC PARAMETERS ADOPTED IN THE TEST				
About SMESs (for $\forall k \in \mathcal{K}$)	$P_{k,max}^S / P_{k,max}^{dS}$ (kW)	300/300	$S_{k,Mod}$ (kVA)	300
	e_i^s / e_i^d	0.95/0.95	E_k (kW·h)	750
	$SOC_{k,min} / SOC_{k,max}$	0.1/0.9	μ_i (L/ Δt)	8
About DR (for $\forall i \in \mathcal{N}_{DR}$)	$T_{i,DU,max}$ (h)	4	$T_{i,DU,min}$ (h)	2
	$T_{i,IN,max}$ (h)	3	$T_{i,DR,max}$ (h)	8
	$\tau_{i,min}^{DR} / \tau_{i,max}^{DR}$	0.4/0.6	$T_{i,pdu}$ (h)	2
	b_1, b_2 for commercial loads	0.35, 0.15	b_1, b_2 for residential loads	0.7, 0.3
About FFGs (for $\forall f \in \cup_{i \in \mathcal{N}} \mathcal{F}(i)$)	$P_{f,max}^F$ (kW)	200	$Q_{f,max}^F$ (kVar)	200
	$S_{f,FFG}$ (kVA)	250	σ_f (L/kW· Δt)	0.282
Uncertainty set	$\Delta \tilde{P}_{id}^{OL}$ and $\Delta \tilde{P}_{id}^{POL}$	$0.2 \tilde{P}_{id}^{OL}$	$\Delta \tilde{P}_{id}^{REG}$ and $\Delta \tilde{P}_{id}^{REG}$	$0.2 \tilde{P}_{id}^{REG}$
Others	Δt (h)	1	D (h)	24
	$\kappa_1, \kappa_2, \kappa_3$	0.1618, 0.0679, 0.7703		

feeder system is used as the IDS [24]. The model is coded on the MATLAB R2020b platform with the YALMIP toolbox [30] and the MILPs are solved by Gurobi v9.1.1 on a computer with an Intel Core i5 8250U CPU and 12 GB RAM.

A. Test System and Scenario

We focus on the cases where an IDS loses connections to the normal power source for a long time in this paper. A wind-based REG with a rated power of 0.8 MW acts as the main source that powered the IDS under normal circumstances and is assumed to be dropped from the IDS due to some major disaster in the test, as shown in Fig. 3. For simplicity, we assume that no other faults exist on branches or nodes inside the IDS and that the topology of the IDS is fixed during scheduling. Thus, tie lies originally in the test system are removed, given that network reconfiguration is out of our scope. A light demand level is assumed for the IDS and the rated load at each node in the IDS has been shrunk to one-fifth of the original value in [24]. The priority weights of loads are randomly assigned from 1 to 5. Types of loads (commercial or residential) are arbitrarily set and eight of them are selected as participants of DR. The residential and commercial load profiles of Los Angeles, CA, USA, obtained from [31], are used to depict the IDS load, and the wind power profile, obtained from CAISO [32], is used to depict the REG output in the test. The day-ahead forecasted loads and REG output are drawn in Fig. 4 as multipliers of the rated values. Two FFGs for back-up use are assumed in the IDS,

each of which has a 200 kW/250 kVA capacity [33]. The SMESs in the test comprises one Carr (e.g., a tractor) and two 300 kW/750 kW·h Mods, all of which are initially located at node 1. The initial SOC of the two Mods is set as 0.5. The Carr can carry one or both of the Mods simultaneously, and 1 time span is assumed for it to travel between node 1 and the stranded REG. The budgets of uncertainty in (17) are set as 24. κ_1, κ_2 , and κ_3 are determined by AHP, based on the assumption in the test that serving as many loads as possible is far more important than saving the consumed fuel and reducing the DR executions. The main parameters are listed in Table II.

B. Solution and Analysis

Based on the above parameters, the proposed two-stage RO model is solved after three iterations using the method in Section IV. The obtained first-stage decisions, including the states of nodes being picked up or executed DR and traveling behaviors of SMESs, are shown in Fig. 3, Fig. 5, and Fig. 7. By substituting the first-stage results and the worst-case scenario obtained from the final iteration into the second-stage problem, i.e., **SP1** while the uncertainty is realized and u is known, the second-stage results under the worst-case scenario, including the power outputs of the Mods and FFGs and the load reduction of DR, are solved and shown in Fig. 5 - Fig. 7.

Twenty-four of the IDS nodes, accounting for approximately 80% of the total demand, are picked up and served during the scheduling, as shown in Fig. 3, while the remaining demand of the other nine nodes is “abandoned”. Several round trips of the Mods are completed by the Carr between the IDS and the external REG, as shown in Fig. 5 (a); and as expected, the two Mods are in a charging state when located at the REG and in a discharging state at the IDS to realize the transportation of energy between the two locations. In addition, it is observed from Fig. 5 (b) that, much of the time (during time spans 8 - 21), the two Mods work alternately as the auxiliary source with the FFGs to supply the IDS continuously. For the two FFGs, since the weight value of serving demand κ_3 is set much higher than that of fuel consumption κ_1 in the objective function, a full-power output is mostly realized for both of the FFGs, as shown in Fig. 6. DR is executed at nodes 4, 14, 24, and 25. It seems that commercial loads are preferred to the execution of DR due to their lower rebound effect than residential loads. We draw the actual hourly total demand served during the scheduling and its value without DR in Fig. 8, which shows an interesting coordination between SMESs and DR.

From the total load perspective, four periods can be recognized as the load reduction due to DR, as shown in Fig. 8. For *Period I*, a tiny reduction occurs because, if without DR, the power demand would slightly exceed the available power of the two FFGs in time span 7 when the Mods have still been on the trip. Thus, DR is executed at node 14 to cope with that slight power shortage issue. For *Periods II* and *III*, as shown in Fig. 7, DRs are executed by commercial loads, which have a gain of energy payback below 100%, and load reduction occurs mainly resulting from the purpose of saving energy to use for the following peak demand during time spans 16 - 17. Specifically, during *Period II* or time spans 9 - 11, Mod 1 works as the only auxiliary source except for the FFGs. Saving energy is required for Mod 1 because sufficient energy should be kept to confront that peak and supply the IDS after the peak (as shown in Fig. 5,

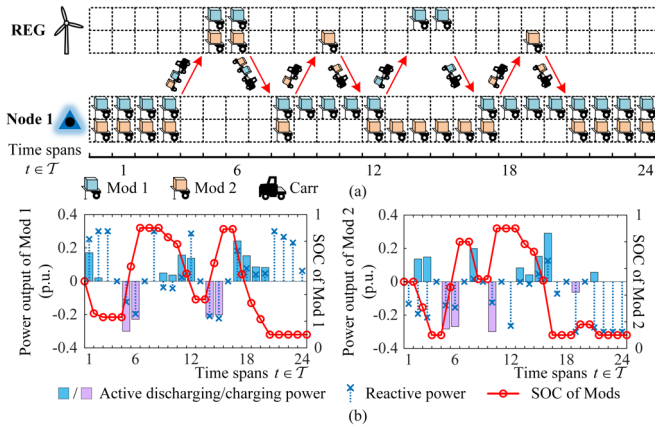


Fig. 5. Scheduling results of (a) traveling behaviors of SMES; and (b) power outputs and SOC of Mods 1 and 2 under the worst-case scenario. The base power is set as 1 MVA.

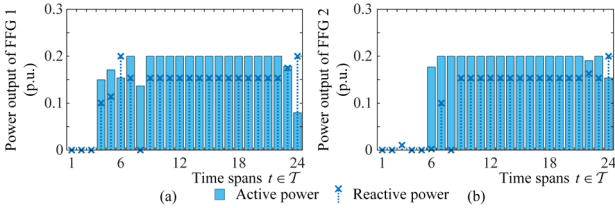


Fig. 6. Scheduling results of power outputs of FFGs at (a) nodes 7 and (b) node 8 under the worst-case scenario.

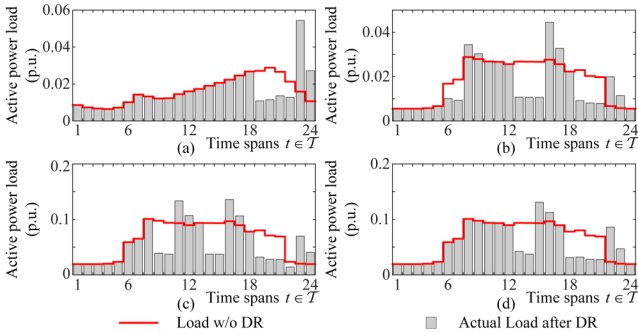


Fig. 7. Scheduling results of DR executions at (a) node 4, (b) node 14, (c) node 24, and (d) node 25.

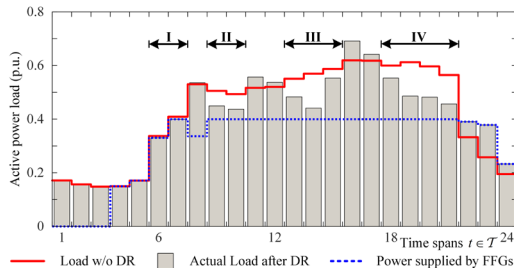


Fig. 8. The total demand served in the IDS without DR and after DR. a near full discharge of Mod 1 is observed around time span 18). In addition, even though Mod 1 is carried soon to the REG and charged, during time span 14 - 15, the power output of the REG is limited and below the full charging power of Mod 1 under the obtained worst case where only 80% of the forecasted power is available during this period. During *Period III*, Mod 2 acts as the only auxiliary source. Similarly, saving energy is important for it to confront the upcoming peak demand, and conservative operation is required during this period. Then, after the peak demand, during *Period IV*, the available energy of the two Mods is limited. As shown in Fig. 5 (b), Mod 2 is charged at the

TABLE III
COMPARISON OF RESULTS AMONG CASES 1 TO 4

Case	$\Psi_{11}/\Psi_{1,max}$	$\Psi_{12}/\Psi_{1,max}$	$\Psi_2/\Psi_{2,max}$	$\Psi_3/\Psi_{3,max}$
1	0.0207	0.6924	0.4205	0.1330
2	0.0207	0.6184	0	0.1939
3	0	0.7813	0.1637	0.1975
4	0	0.7455	0	0.2278

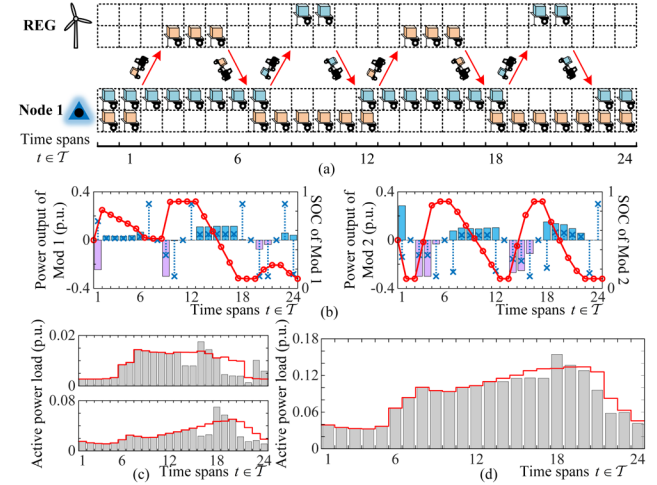


Fig. 9. Scheduling results of (a) traveling behaviors of SMES, (b) power outputs and SOC of Mods 1 (left) and 2 (right), (c) DR executions at nodes 15 (upper) and 32 (lower), and (d) the total demand served without DR and after DR under the special case. The same legend as Fig. 5 - Fig. 8 is used.

REG only to a low level due to the REG's very limited power under the worst case. Both of the Mods use up their energy at the end of this period, and if without DR, as shown by the part between the red line and the blue dashed line in Fig. 8, *Period IV* cannot be successfully rid through due to the greater energy shortage.

C. Comparison among Cases

Based on the above test system, the effectiveness of our proposed method is further demonstrated by comparison among the following cases. *Case 1*: SMES and DR (*i.e.*, the proposed method and the analysis in the previous subsection). *Case 2*: SMES without DR. *Case 3*: Stationary Mods and DR. *Case 4*: Stationary Mods without DR.

The revisions to the model for realizing the above cases are given in the electronic appendix of this paper [34]. For *Cases 3* and *4*, Mod 1 and Mod 2 are fixed at their initial location, *i.e.*, at node 1. The results of the terms in the objective function under the four cases are given in Table III. By using the proposed method that coordinates the scheduling of SMES and DR in the IDS operation, the lowest weighted abandoned demand is realized under *Case 1*, which is decreased by 31.4% and 32.7% compared with scheduling SMES and DR alone under *Case 2* and *Case 3*, respectively, and especially by 41.6% compared with *Case 4*. In brief, comparing *Case 2* to *Case 1* (or *Case 4* to *Case 3*), DR enables more loads to be served by aptly relieving the operating stress in terms of power and energy shortage, as analyzed before, though it also brings more fuel consumed for FFGs generation under the preset $\kappa_1, \kappa_2, \kappa_3$. By using SMES, comparing *Case 3* with *Case 1* (or comparing *Case 4* with *Case 2*), more loads are served with less fuel consumption due to the increased power capacity and the energy supplemented from outside.

In addition, a *special case* is given as "SMES and DR

without FFGs”, *i.e.*, the IDS losing the FFGs. As shown by the result in Fig. 9 (a) and (b), a continuous power supply to the IDS is realized for the whole time by the alternate work of the two Mods of SMCESS. This enables eight of the nodes be served during the scheduling even without FFGs, with the help of DR executed at nodes 15 and 32, as shown in Fig. 9 (c) and (d).

VI. CONCLUSION

Frequently occurring catastrophic events currently drive the requirement to enhance the power system survivability. In this paper, we propose a two-stage robust scheduling strategy to strengthen the IDS survivability by coordinating the two kinds of smart grid technologies, namely, SMCESSs and DR. With the survivability-oriented purpose, the SMCESSs are scheduled to construct non-wires links reconnecting the external stranded sources and the IDS, which enable the successive supplement of energy. Through alternate work, an additional continuous power supply can also be realized. DR is coordinated and scheduled to relieve the operating stress of the IDS in time. In addition to the commonly seen power shortage relief, the relief to the energy shortage for IDS is also recognized to realize the proper energy use for the demand beyond the touch of FFGs in the IDS under limited available energy. The numerical results show the effectiveness and advantages of the proposed strategy.

REFERENCES

- [1] “Electric power system resiliency: Challenges and opportunities,” Electric Power Research Institute (EPRI). Palo Alto, CA, USA, Tech. Rep. 3002007376, Feb. 2016.
- [2] “Enhancing distribution resiliency: Opportunities for applying innovative technologies,” Electric Power Research Institute (EPRI). Palo Alto, CA, USA, Tech. Rep. 1026889, Jan. 2013.
- [3] “Improving electric grid reliability and resilience: Lessons learned from Superstorm Sandy and other extreme events,” The GridWise Alliance, Jun. 2013. [Online]. Available: <http://gridwise.org/superstorm-sandy-report/>
- [4] Z. Bie, Y. Lin, G. Li, and F. Li, “Battling the extreme: a study on the power system resilience,” *Proc. IEEE*, vol. 105, no. 7, pp. 1253-1266, Jul. 2017.
- [5] X. Wang, Z. Li, M. Shahidehpour, and C. Jiang, “Robust line hardening strategies for improving the resilience of distribution systems with variable renewable resources,” *IEEE Trans. Sustain. Energy*, vol. 10, no. 1, pp. 386-395, Jan. 2019.
- [6] M. Nazemi, M. Moeini-Agtaie, M. Fotuhi-Firuzabad, and P. Dehghanian, “Energy storage planning for enhanced resilience of power distribution networks against earthquakes,” *IEEE Trans. Sustain. Energy*, vol. 11, no. 2, pp. 795-806, Apr. 2020.
- [7] W. Yuan *et al.*, “Robust optimization-based resilient distribution network planning against natural disasters,” *IEEE Trans. Smart Grid*, vol. 7, no. 6, pp. 2817-2826, Nov. 2016.
- [8] S. Ma, S. Li, Z. Wang, and F. Qiu, “Resilience-oriented design of distribution systems,” *IEEE Trans. Power Syst.*, vol. 34, no. 4, pp. 2880-2891, Jul. 2019.
- [9] M. H. Amirioun, F. Aminifar, and H. Lesani, “Resilience-oriented proactive management of microgrids against windstorms,” *IEEE Trans. Power Syst.*, vol. 33, no. 4, pp. 4275-4284, Jul. 2018.
- [10] S. Lei, C. Chen, H. Zhou, and Y. Hou, “Routing and scheduling of mobile power sources for distribution system resilience enhancement,” *IEEE Trans. Smart Grid*, vol. 10, no. 5, pp. 5650-5662, Sep. 2019.
- [11] S. Yao, P. Wang, X. Liu, H. Zhang, and T. Zhao, “Rolling optimization of mobile energy storage fleets for resilient service restoration,” *IEEE Trans. Smart Grid*, vol. 11, no. 2, pp. 1030-1043, Mar. 2020.
- [12] S. Lei, C. Chen, Y. Li, and Y. Hou, “Resilient disaster recovery logistics of distribution systems: co-optimize service restoration with repair crew and mobile power source dispatch,” *IEEE Trans. Smart Grid*, vol. 10, no. 6, pp. 6187-6202, Nov. 2019.
- [13] C. Chen, J. Wang, F. Qiu, and D. Zhao, “Resilient distribution system by microgrids formation after natural disasters,” *IEEE Trans. on Smart Grid*, vol. 7, no. 2, pp. 958-966, Mar. 2016.
- [14] M. R. Kleinberg, K. Miu, and H. Chiang, “Improving service restoration of power distribution systems through load curtailment of in-service customers,” *IEEE Trans. Power Syst.*, vol. 26, no. 3, pp. 1110-1117, Aug. 2011.
- [15] C. Chen, J. Wang, and D. Ton, “Modernizing distribution system restoration to achieve grid resiliency against extreme weather events: an integrated solution,” *Proc. IEEE*, vol. 105, no. 7, pp. 1267-1288, Jul. 2017.
- [16] J. Nelson, N. G. Johnson, K. Fahy, and T. A. Hansen, “Statistical development of microgrid resilience during islanding operations,” *Appl. Energy*, vol. 279, Dec. 2020, Art. no. 115724.
- [17] Y. Kuang *et al.*, “A review of renewable energy utilization in islands,” *Renew. Sustain. Energy Rev.*, vol. 59, pp. 504-513, Jun. 2016.
- [18] W. Wang, X. Xiong, Y. He, J. Hu, and H. Chen, “Scheduling of separable mobile energy storage systems with mobile generators and fuel tankers to boost distribution system resilience,” unpublished paper, 2020. [Online]. Available: <http://arxiv.org/abs/2012.03209>
- [19] A. L. A. Syrri and P. Mancarella, “Reliability and risk assessment of post-contingency demand response in smart distribution networks,” *Sustain. Energy, Grids and Netw.*, vol. 7, pp. 1-12, Sep. 2016.
- [20] C. Gouveia, J. Moreira, C. L. Moreira, and J. A. Peças Lopes, “Coordinating storage and demand response for microgrid emergency operation,” *IEEE Trans. Smart Grid*, vol. 4, no. 4, pp. 1898-1908, Dec. 2013.
- [21] “NYISO 2019 annual report on demand response programs,” New York Independent System Operator, Inc. (NYISO), Rensselaer, NY, USA, Jan. 2020. [Online]. Available: <http://www.nyiso.com/documents/20142/10360921/NYISO-2019-Annual-Report-on-Demand-Response-Programs.pdf/25a998b4-d134-f5f5-2a27-a17568e9b3c7>
- [22] W. Wang, X. Xiong, C. Xiao, and B. Wei, “A novel mobility model to support the routing of mobile energy resources,” unpublished paper, 2020. [Online] Available: <http://arxiv.org/abs/2007.11191>
- [23] N. Motegi, M. A. Piette, D. S. Watson, S. Kiliccote, and P. Xu, “Introduction to commercial building control strategies and techniques for demand response,” Lawrence Berkeley National Laboratory, Berkeley, CA, USA, Rep. LBNL-59975, May 2007.
- [24] M. E. Baran and F. F. Wu, “Network reconfiguration in distribution systems for loss reduction and load balancing,” *IEEE Trans. Power Del.*, vol. 4, no. 2, pp. 1401-1407, Apr. 1989.
- [25] D. Bertsimas and M. Sim, “The price of robustness,” *Oper. Res.*, vol. 52, no. 1, pp. 35-53, Jan.-Feb. 2004.
- [26] X. Chen, W. Wu, and B. Zhang, “Robust restoration method for active distribution networks,” *IEEE Trans. Power Syst.*, vol. 31, no. 5, pp. 4005-4015, Sept. 2016.
- [27] B. Zeng and L. Zhao, “Solving two-stage robust optimization problems using a column-and-constraint generation method,” *Oper. Res. Lett.*, vol. 41, no. 5, pp. 457-461, 2013.
- [28] H. Konno, “A cutting plane algorithm for solving bilinear programs,” *Math. Program.*, vol. 11, pp. 14-27, 1976.
- [29] V. Gabrel, M. Lacroix, C. Murat, and N. Remli, “Robust location transportation problems under uncertain demands,” *Discrete Appl. Math.*, vol. 164, pp. 100-111, Feb. 2014.
- [30] J. Löfberg, “YALMIP: A toolbox for modeling and optimization in MATLAB,” in *Proc. IEEE Int. Symp. Comput. Aided Control Syst. Des.*, 2004, pp. 284-289
- [31] Office of Energy Efficiency & Renewable Energy (EERE). Commercial and Residential Hourly Load Profiles for all TMY3 Locations in the United States. [Online]. Available: <http://openei.org/datasets/dataset/commercial-and-residential-hourly-load-profiles-for-all-tmy3-locations-in-the-united-states>
- [32] California ISO. Today’s outlook. [Online]. Available: <http://www.caiso.com/TodaysOutlook/Pages/supply.html>
- [33] Caterpillar Inc. 200 kW diesel generator set. Accessed: Feb. 13, 2021. [Online]. Available: http://www.cat.com/en_US/products/new/power-systems/electric-power/diesel-generator-sets/106462.html
- [34] W. Wang, X. Xiong, Y. He, and H. Chen. Appendix for “Robust Survivability-Oriented Scheduling of Separable Mobile Energy Storage and Demand Response for Isolated Distribution Systems”. [Online]. Available: http://drive.google.com/file/d/1S1239unR8221mjv9xGhGLdOQCJ_WA/Eu/view?usp=sharing